This is a repository copy of *Review of recent progress in nanoscratch testing*.

White Rose Research Online URL for this paper:
http://eprints.whiterose.ac.uk/84183/

Version: Accepted Version

Article:

A review of recent progress in nano-scratch testing

B.D. Beake[1,3], A.J. Harris[1] and T.W. Liskiewicz[2]

[1] Micro Materials Ltd., Willow House, Ellice Way, Yale Business Village,

Wrexham, LL13 7YL, UK

[2] Institute of Engineering Thermofluids, Surfaces & Interfaces, School of Mechanical

Engineering, University of Leeds, Woodhouse Lane, Leeds, LS2 9JT, UK

[3] Ben@micromaterials.co.uk

Abstract

Nano-scratch testing, as an important technique for the assessment of the mechanical failure behaviour and adhesion strength of ceramic coatings and a simulation tool of single asperity contact in tribological experiments, is increasingly becoming an established nanomechanical characterisation method. This paper reviews recent work in nano-scratch testing in different engineering applications including thin ceramic films, automotive organic coatings, chemical–mechanical polishing and bio-materials. In the main part of the paper nano-scratch results from experiments performed using NanoTest systems fitted with tangential force sensors and spherical indenters as scratch probes are presented and discussed. The type of nano-scratch tests described include (i) constant load nano-scratches (ii) ramped load nano-scratch tests and (iii) multi-pass repetitive unidirectional constant load nano-scratch tests (nano-wear). The results are discussed in terms of critical load sensitivity to intrinsic and extrinsic factors, impact of scan speed and loading rate, influence of probe radius and geometry, estimation of tip contact pressure, influence of surface roughness and film stress and thickness, and finally role of ploughing on friction evolution.

1. Introduction

Over the last 25 years commercial nanomechanical testing instruments have expanded the range of their test techniques beyond simple nanoindentation to include capability for nanotribological measurements such as nano-scratch and nano-wear testing which has consequently greatly expanded their range of applications. Nano-scratch testing in particular is increasingly becoming an established nanomechanical characterisation method. It is mainly used for adhesion strength and mechanical failure modes measurement of ceramic coatings however it also brings interesting capabilities for nano-scale characterization of bulk materials. Nano-scratch testing overcomes some of the limitations of atomic force microscopy (AFM) in terms of measurement stability and excessive tip wear on hard samples and is an important tool in simulation of single asperity contact in tribological experiments. It is a flexible method, which can be easily tailored to represent different application scenarios by using various types of tip materials and geometries as well as different test kinetics with a constant or ramped applied load in a single or repetitive scratch mode.

In the design of coatings for improved tribological performance, a key issue to be resolved is the relationship between the coating mechanical properties and its adhesion to the substrate. It has been found that the mechanical response of a coated component is underpinned by the film/substrate system deformation behaviour rather than the adhesion strength alone[1-11]. Both scratch resistance and interfacial toughness/adhesion under light and heavy loaded sliding contact can be assessed through nano-scratch experiments. Moreover, the progressive load nano-scratch test enables film performance throughout the load range to be assessed in a single test.

The majority of published work in nano-scratch testing area relates to establishing mechanical parameters of various coating/substrate systems. Roy et al. used nano-scratch test to characterize the interfacial adhesion of amorphous SiCN thin films deposited by PECVD method on Cu/Si substrates[12]. The authors showed a relationship between the stresses in the coating and the cracking/buckling behaviour of the film observed experimentally which was then further analysed by three-dimensional finite element model. A multilayer coating system Au/NiCr deposited on Al_2O_3 substrate was studied by Tang et al[13]. Based on experiments, the coating deformation process was divided into three stages and it was found that plastic deformation dominated over elastic deformation before the film failure for this metallic system. Various coating systems were investigated by Beake et al. by means of nano-scratch method[10-11,14-19]. In ref. 11 high resolution Scanning Electron Microscopy (SEM) has been used in conjunction with progressive load nano-scratch testing and nanoindentation to investigate TiFeN, TiN and TiFeMoN films behaviour in highly loaded sliding and mechanical properties. It has been found that softer films exhibited lower ratios of hardness to modulus (H/E_r) and films with $H/E_r \leq 0.11$ possessed a more optimum combination of mechanical properties for applications where they are exposed to high shearing forces and strain in the film. In Refs. 14,17,19 much thinner (5, 20 and 80 nm) ta-C films deposited on Si (100) were assessed for potential applications in Silicon-based micro-systems when mechanical contact occurs. Small scale fretting, nano-scratch and nanoindentation experiments were performed using spherical indenters to investigate the influence of the mechanical properties and phase transformation behaviour of the silicon substrate on tribological performance of films. A clear correlation between the fretting and nano-scratch tests was found despite the differences in contact pressure and failure mechanism.

Nano-scratch testing has been successfully used in other applications than coated systems. Noh et al. looked at the scratch characteristics of automotive organic coatings using nano-

scratch tests[20]. The results showed a close correlation between the scratch resistance data obtained from car-wash experiments and nano-scratch tests and confirmed that mechanical properties, including scratch resistance, are improved with increased crosslinking networks in the coatings. In work carried out by Fu et al. [21], nano-scratch experiments were performed using AFM in deionized water and a slurry to investigate mechanical aspects of material removal process in chemical–mechanical polishing. Significantly deeper scratches were generated in slurry than in DI water, which was attributed to a soft passivation layer generated during chemical interactions on the copper surface. Nano-scratch method has been also increasingly employed recently in bio-materials testing, where, amongst other cases, it was used to evaluate the wear behaviour of human root canal dentin [22], investigate tribological properties of PMMA-based bone cements [23] or compare mechanical behaviour of materials used in total hip replacement components [24].

Although an international standard for nanoindentation now exists, nano-scratch testing is yet to be standardised despite being in increasingly common use. Project partners in the EU projects NANOINDENT [25] and NANOINDENT-PLUS [26] have been performing round robin investigations to deepen our understanding of the technique as a first step towards a test standard detailing the recommended experimental protocol and data interpretation in nano-scratch testing. In this paper nano-scratch tests on coating and bulk materials using single-pass constant and ramped loads method as well as multi-pass repetitive unidirectional constant load method are evaluated including studies on TiN films performed within the NANOINDENT project. The results are discussed in terms of critical load sensitivity to intrinsic and extrinsic factors, impact of scan speed and loading rate, influence of probe radius and geometry, estimation of tip contact pressure, influence of surface roughness and film stress and thickness, and finally role of ploughing on friction evolution.

2. Experimental methods

The nano-scratch tests described include (i) constant load nano-scratches (ii) ramped load nano-scratch tests and (iii) multi-pass repetitive unidirectional constant load nano-scratch tests (nano-wear). The progressive load nano-scratch tests were performed as a topography-progressive load scratch-topography multi-pass procedure. The progressive load ''3-scan'' scratch tests, constant load single scratches and repetitive scratch tests (nano-wear) were all performed using NanoTest systems (manufactured by Micro Materials, Wrexham, UK) fitted with tangential force sensors and spherical indenters as scratch probes. The end radii of the scratch probes were calibrated by nanoindentation. The design of the NanoTest combines high frictional sensitivity with sufficiently high lateral stiffness for accurate friction determination. Data were corrected in the NanoTest software to allow estimation of mean contact pressure by an in situ method without recourse to post-test imaging of scratch tracks. Table 1 summarises the systems studied and the scratch probe radii used.

Table 1

Material system	Film thickness (µm)	Scratch probe radius (µm)	Reference
TiSiN on Si	0.4-1.1	3.0	10
a-C:H and Si:a-C:H on glass	0.14-0.61	~0.5, 3	15
ta-C on Si	0.005-0.08	1.1, 3.1, 4.6, 9.0	14,17,19
a-C on Si	0.2-1.1	4.0	16
TiN on tool steel	0.5-1.5	3.1, 4.4	18
TiFeN, TiFeMoN and TiN on Si	0.9-1.5	~0.5	11
Si(100)	(bulk)	4.6	24
Ti6Al4V, CoCr, 316L stainless steel	(bulk)	3.7	27

3. Results and Discussion

3.1. Critical load sensitivity to intrinsic and extrinsic factors

Steinmann and co-workers reported that the critical load in the macro-scale scratch test could be influenced by a range of extrinsic and intrinsic factors with intrinsic factors including scratching speed, loading rate, tip radius and extrinsic factors such as substrate hardness, and the roughness, thickness and friction of the coating [5]. More recently it has been shown that in addition to these factors the mechanical properties of the coating also play a critical role in nano-scratch testing, with even quite small changes in H/E capable of altering the locus of film failure relative to the moving probe in hard nitride films [10,11]. The lateral stiffness of the

instrument is also important. If the test instrument can combine high frictional sensitivity with sufficiently high (i.e. optimised) lateral stiffness then the probe traces remain very smooth until film failure. In contrast if the instrument has insufficient lateral stiffness the scratch tracks are wavy on all but the smoothest samples. A sensitive friction force capability in the nano-scratch test is highly desirable for several reasons including (i) reliable quantitative friction data to be obtained, (ii) separate the interfacial and ploughing contributions to the total measured friction (iii) clear identification of the onset of wear.

3.2. Scan speed and loading rate

The variation in critical load in the macro-scale scratch test on a 3.5 µm thick CVD TiC coating on steel with a 200 µm radius diamond with scan speed and loading rate has been studied [5]. It was found that for this system the critical load decreased at lower loading rate and increased at lower scratching speed. However, provided tests were performed at a constant dL/dx ratio (the increase in load per unit scratch distance where L = normal load and x = scratch distance) the critical load was approximately constant within the precision of their measurements. Since a reduction in critical load was found when dL/dx decreases it was recommended tests that be done with a fixed dL/dx of 10 N/mm. Steinmann et al suggested that the probability of encountering defective adhesion within a certain load range increases when dL/dx decreases, resulting in a decreased critical load. However, this explanation may not apply for highly homogeneous coatings that do not fail by selective failure of poorly adhering regions and so exhibit very consistent L_c values, and also does not consider the possibility of cohesive failure.

The influence of loading rate and scan speed on the critical load in the nano-scratch test has been investigated for DLC and Si-doped DLC coatings on glass that show clear film failure

[15]. There was considerably less sensitivity to these scan parameters than has observed in macro-scale scratch testing. When testing these samples at the nano-scale, no marked dependence on critical load was found on (1) scratching speed, (2) loading rate, or (3) (dL/dx) when dL/dx is much less than 1 N/mm, whilst critical loads only slightly increase at higher dL/dx (1-5 N/mm). Recently Beake and co-workers have reported little clear variation in critical load for failure of a 80 nm ta-C film on Si over a 100 fold range of dL/dx [19]. These results suggest that nano-scratch tests under significantly different loading conditions can be compared directly.

3.3. Topography-progressive load scratch-topography multi-pass scratch tests

An improvement on the basic nano-scratch test is the 3-scan procedure (topography scan - progressive scratch - topography scan) that enables identification of failure mechanisms, the role of stress in particular, in more detail. The first reported multi-pass test of this type was described in detail by Wu and co-workers from IBM in 1989 [28,29]. In 2006 Beake and co-workers showed that by removal of the instrument compliance contribution to the measured deformation the true nano-scratch and nano-wear depth data could be displayed after levelling [10]. By performing three-scan progressive load nano-scratch tests it is possible to determine the critical load for the onset of non-elastic deformation since this is the load at which the residual scratch depth is no longer zero. The mean pressure at this point can be used as an estimate of the yield pressure.

3.4. Influence of probe radius and geometry

Material behaviour in the nano-scratch test is critically dependent on the radius of the test probe. Periodic calibration of the indenter radius by nanoindentation is necessary to determine the effective radius and ensure the calibration remains accurate. If possible, this

calibration should be done with the probe in the same loading head. For bulk materials transitions occur when critical pressures are reached, as in nanoindentation. The critical load at the onset of non-elastic deformation of fused silica appears to occur when a critical pressure of about 8 GPa is reached. Assuming constant mean pressure (for a bulk material displaying no indentation size effects) leads to power law dependence with exponent of two for the variation of the critical load with probe radius. For coatings the behaviour may be more complex when failures occur not solely at a critical pressure but are also associated with exceeding a critical bending strain in the coating.

Sphero-conical probes with end radius typically 1-10 μm are commonly used in nano-scratch testing. Figure 1 shows the variation in the critical load for the total film failure of an 80 nm FCVA ta-C film on Si wafer. The critical load follows a power law dependence on the probe radius of the type shown in equation 1 where a is a measure of the effective adhesion strength in the nano-scratch test. The best fit curve to the data in figure 1 is given by a curve of $y = 8.4x^{1.76}$.

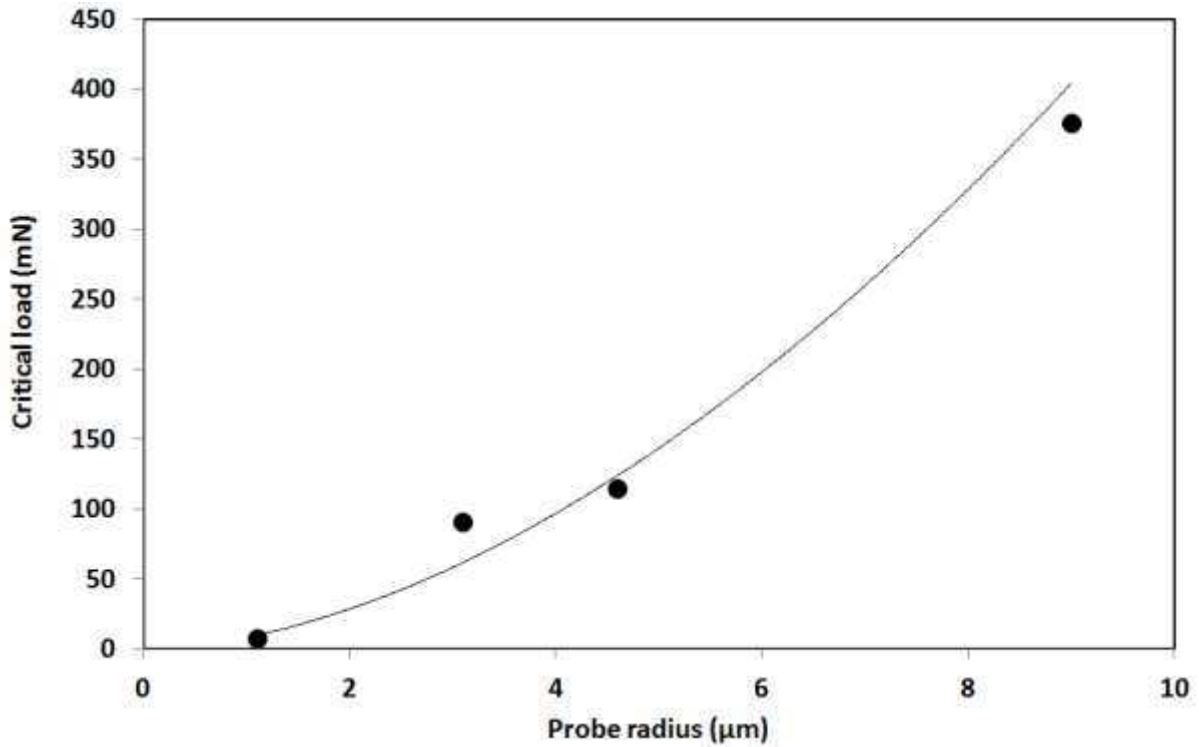$$L_c = aR^m \qquad \text{[Eqn. 1]}$$

Figure 1. Influence of probe radius on the critical load for total film failure of 80 nm ta-C films on Si

It may not be possible to cause complete film failure when the test probe radius is too great or the test instrumentation has a relatively small maximum load. A ~5 μm end radius represents an effective choice ensuring that coating failure is observed within the force range of several commercial instruments but without risking rapid blunting of the indenter due to repeat scanning that can be observed when sharper probes are used (such as Berkovich indenters), especially when scratching hard and rough coatings. A limitation of the very low force range of AFM and some nanoindenter designs is the rapid wear of the sharp probes needed.

The use of the spherical indenters has the additional advantage that the contact pressure analysis described below can be directly applied to the nano-scratch data, provided the instrument software has the capability to remove the contribution of instrument compliance,

sample slope and roughness from the measured deformation data so that true nano-scratch and nano-wear depth data is displayed.

3.5. Contact pressure

The progressive load multi-pass scratch technique has been improved by an analytical approach which obtains accurate scratch depth data after correction of the raw data for the contribution from instrument compliance, sample topography and sample slope [9,17]. The method described in reference 17 enables the yield stresses and the pressure required for the failure of the film to be estimated from contact mechanics, assuming the geometry of indentation, provided spherical indenters are used. By using spherical probes the contact depth (h_p) in an indentation contact is given by

$$h_p = (h_t + h_r)/2 \qquad \text{[Eqn. 2]}$$

where h_p is the contact depth, h_t is the on-load scratch depth and h_r is the residual depth from the final scan. The contact radius (a) is determined from Equation 3, where R is the indenter radius.

$$a = \sqrt{(2Rh_p - h_p^2)} \qquad \text{[Eqn. 3]}$$

$$P_m = L/\pi a^2 \qquad \text{[Eqn. 4]}$$

The contact pressure, P_m, at any point along the scratch track is given by equation 4, where L is the applied load. To apply this approach to the nano-scratch data it is necessary to assume that:

(1) the presence of a tangential load does not influence the pressure distribution too greatly so that the measured friction coefficient is well below 0.3;

(2) the radius of the indenter is constant ;

(3) the sliding speed is sufficiently slow and contact sufficiently close to elastic that the load is supported on the rear of the indenter;

(4) the indenter can reach the bottom of the scratch track in the final topographic scan.

These conditions can be met in the nano-scratch test, although the approximation becomes less valid as the geometry moves away from Hertzian conditions due to increasing friction or plasticity. The methodology has been validated for thin films on Silicon wafers with good agreement between (i) scratch hardness independently determined from optical measurements of scratch widths (ii) contact pressures for film and substrate yield events. The approach described above can also provide an estimate of the contact pressure during the progressive load nano-scratch test, at least at low contact forces where the friction coefficient is sufficiently low. It can provide an estimate of the mean contact pressure required to produce plastic deformation.

Nano-scratch testing has been applied to the study of the durability of metallic alloys (Ti6Al4V, CoCr and 316L stainless steel) that are increasingly popular for biomedical and other advanced applications [27]. In order to develop improved mechanistic understanding for reliable artificial joint design, it is necessary to investigate the mechanical and tribological properties of biomedical materials at the relevant contact scale as these properties can be highly size dependent. Hardness and yield stress increase as the length-scale of the contact is reduced ("smaller is stronger") [30-32]. Reported macroscopic yield stresses of these biomedical

materials are in the range 0.3-1 GPa, with stainless steel being lowest and Ti6Al4V being highest [33-35]. Mean pressures for measurable plastic deformation in the nano-scratch test (defined by the first point in the final topographic scan showing non-zero depth) were ~2.3 GPa for Ti6Al4V, ~2 GPa for CoCr and ~1 GPa for the 316L stainless steel. This ranking correlates with H^3/E_r^2 which is a measure of the resistance to plastic deformation, and the reported macro-scale yield stresses. The nano-scratch data show higher yield stress at the nano-scale, emphasizing the importance of testing at the relevant scale rather than using bulk values.

3.6. Surface roughness

Beake and co-workers have recently investigated the influence of coating thickness, roughness and the direction of scratching relative to grinding marks on the behaviour of TiN coatings on M42 steel in single and multi-pass nano-scratch (nano-wear) tests [18]. 500 nm and 1500 nm TiN coatings were deposited on M42 steel as this is a model system displaying clear failure with comparative frictional data available from previous macro-scale scratch testing. The critical load for delamination failure was dependent on coating thickness and scratch orientation relative to polishing marks on the surface made prior to coating deposition. The critical load was 22 % lower when scratching perpendicular to the grinding marks than parallel to them. Coating failure was more gradual when the scratch direction was either parallel to or aligned at an intermediate angle to the grinding grooves than when it was perpendicular. The dependence of the critical load on the direction of the nano-scratch orientation relative to the grinding marks is in agreement with literature results [1] in scratch testing of thicker TiN coated HSS with 200 μm probes. The decrease in critical load of ~20-25 % between scratches made across or parallel to grinding grooves for a TiN film with R_a = 0.12 μm in the nano-scratch test is similar to the macro-scale result reported by Larsson et al

who found that below $R_a = 0.1$ μm there was little influence of scan direction but the critical load decreased by over 50% when R_a reaches 0.5 μm [1]. High roughness tends to decrease the critical load but the load carrying capability of higher thickness can have a much greater effect. Despite being much smoother, the critical load on 500 nm TiN was only ~50% of the critical load on the 1500 nm TiN.

3.7. Influence of film stress and thickness

Coatings for mechanical property evaluation by nanoindentation have often been deposited on Silicon as a readily available and smooth choice of substrate. Unsurprisingly, to date many reports of nano-scratch testing have also involved thin coatings deposited on Si substrate. This has the advantage that coatings tend to be smoother but potentially adds some complexity since it has been shown that the combined response of the coating-substrate system can be strongly influenced by the contact-induced phase transformation of the Si substrate. The nanomechanical and nanotribological characterisation of thin films on Si has involved nanoindentation with Berkovich indenters in combination with nano-scratch testing with spherical indenters [10,11,14,16,17,19]. A key motivation was to understand the interplay between film thickness and interfacial toughness for MEMS and other protective thin film applications. The reliability of Si-based MEMS devices is limited by stiction forces when contact occurs. Applying very thin, low surface energy and low stress coatings can alleviate this problem but it is critical that they are deposited optimally.

The film thickness is a key parameter influencing the critical load in the nano-scratch test. In principle, film thickness can have two opposing effects:- 1) thicker films that are harder than the underlying substrate provide more load support and so delay the onset of the substrate deformation that is often the precursor of film failure (higher critical load) 2) thicker films

can be more highly stressed and more easily through-thickness crack and delaminate when deformed (lower critical load) since the driving force for spallation to reduce stored elastic energy is greater.
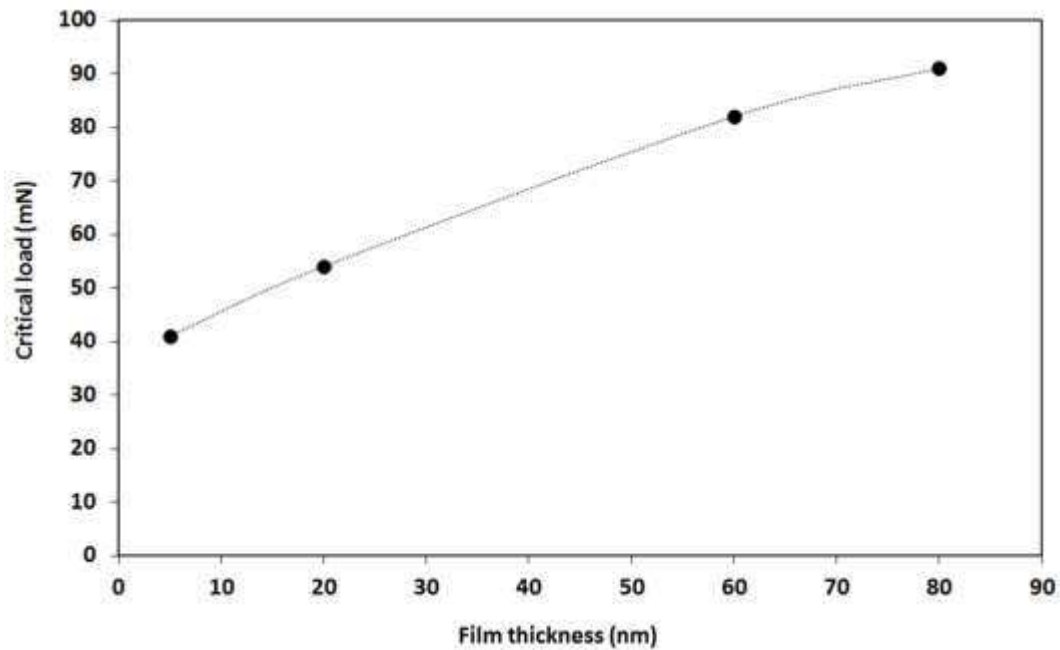

Figure 2. Variation in the critical load for total failure of 5-80 nm ta-C films on Si with their thickness

The relationship between film thickness and critical load can be quite complex in practice. Figure 2 shows how the critical load for film failure varies with the thickness of 5-80 nm FCVA ta-C films on Si when scratched by a R = 3.1 µm probe. The maximum von Mises stress is in the substrate at the critical load. It is deformation of the Si substrate by plasticity and phase transformation which drives the film failure. The increasing critical load with film thickness is due to the ability of the thin films to protect the Si substrate. Nano-scratch studies

on 200-1000 nm a-C films deposited on Si by closed field unbalanced magnetron sputtering (CFUBMS) [16] and 150-600 nm Si:a-C:H films deposited on glass by plasma enhanced chemical vapour deposited (PECVD), [15] have shown that the critical load for total film failure in the nano-scratch test can be strongly correlated with film thickness reflecting enhanced load support and substrate protection.

Provided the films are not too stressed the ratio L_c/t_f can be approximately constant in practice. Si doping during deposition resulted in small mechanical changes of DLC coatings of different thickness on glass but the H/E ratio of the films remained approximately constant. After normalising the critical load by their thickness, as in Figure 3, the films have similar scratch behaviour.
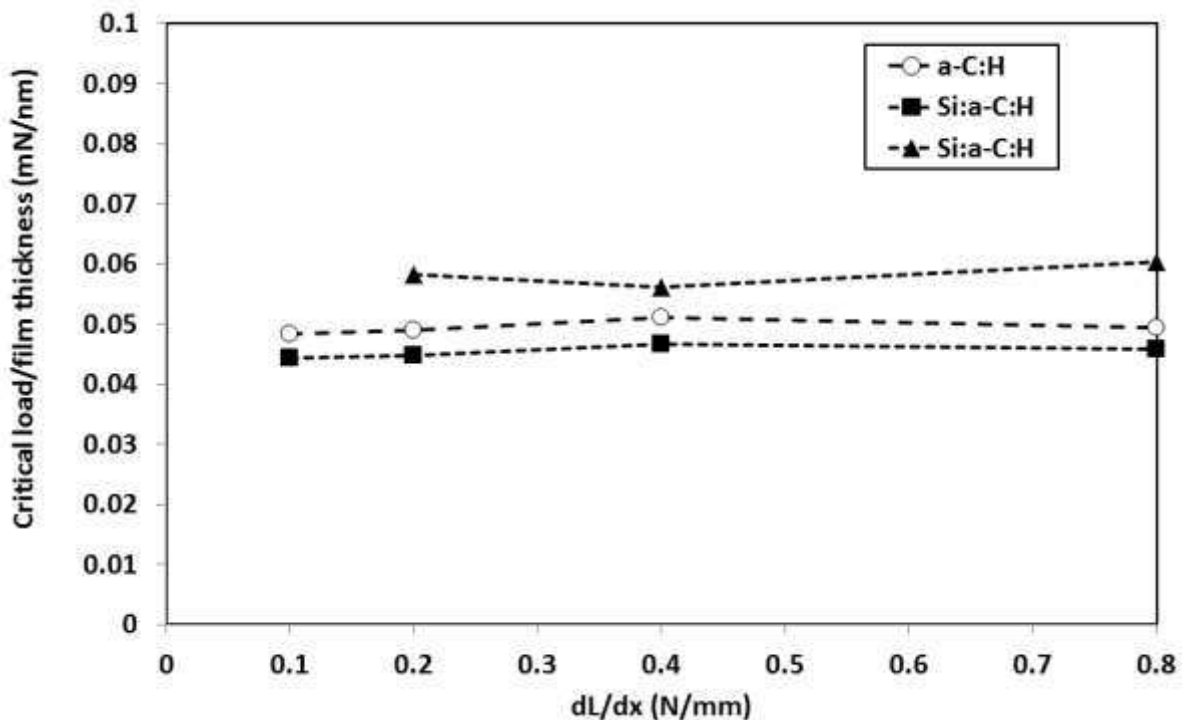

Figure 3. Critical load normalised by film thickness for 141 nm DLC, 366 nm and 614 nm Si-doped DLC films on glass

As part of the NANOINDENT project DLC films were deposited at BAM by CVD on Si to 450 nm and 962 nm thickness without an adhesion-promoting interlayer [25]. Nano-scratch testing with a 3.7 µm probe showed that both films delaminate easily, with the thicker film failing at only half of the critical load of the thinner film to due high stress. Substrate bias during deposition can significantly alter film stress. Shi and co-workers reported nano-scratch data for 200 nm and 1000 nm a-C films deposited with varying substrate bias voltage (-20 to -140V) by CFUBMS [16]. At 200 nm thickness the highest H/E films performed best since the intrinsic stress in the film was relatively low (no recovery spallation and low H/E). For ~1 µm a-C films they observed a general relationship between H/E and the scratch test critical loads. When H/E_r is ~0.09-0.1 there was a tendency of the films to delaminate behind the moving probe at low critical load. Beake and co-workers previously reported a similar correlation for ~0.8 µm Ti-Si-N nanocomposites films on Si [10]. Higher H/E led to higher critical loads for elastic-plastic transition and also for the total film failure occurring in front of the probe. However, when H/E_r was >0.09 film failure was always by tensile failure behind the probe (also described as unloading failure). The high tensile stress behind the probe in the nanoscale scratch test can lead to complete failure for hard films on silicon.

Beake and co-workers recently reported a similar correlation between the mechanical properties of hard 0.9-1.5 µm nitride-based films on Si [11]. At low scratching loads, the mechanical properties of the film itself control nano-scratch behaviour and films with higher H/E and lower plasticity indices are more resistant. At higher scratching load the failure of harder films with $H/E_r > 0.11$ was accompanied by delamination outside the scratch track. It is suggested that hard films with $H/E_r \leq 0.11$ possess a more optimum combination of

hardness and toughness for applications where they will be exposed to high shearing forces and strain in the film in this case is more readily relieved by intergrain cracking.

The results of all these studies show the same trends. For optimum durability in highly loaded sliding contact, when films are deposited to around 1 µm thickness they should not be designed to be as hard and have as high a ratio H/E_r as possible. For high H/E films energy dissipation by mechanisms such as plastic deformation or localised intergranular fracture is less likely during the highly loaded sliding of these hard and elastic films, and ultimately the stored elastic energy is instead relieved by dramatic fracture resulting in a larger delaminated area [11].

3.8. Repetitive nano-wear

More information can be provided by nano-wear tests. Constant load, unidirectional multi-pass scratch testing was first described by Bull and Rickerby in 1989 [58] and has been shown to be an effective low cycle fatigue test. The same approach can be applied to micro- and nano-scratch testing. Constant load nano-wear tests are often used to determine rates of sliding/abrasive wear and investigate the role of fatigue. A typical multi-pass experimental design is shown in figure 4 below. The low-cycle nano-wear experiments can often be much more informative regarding the influence of thin film stress leading to poor adhesion than single scratch tests. When compared to progressive load nano-scratch testing, nano-wear testing has the advantage that the load can be varied to tune the maximum von Mises stress to be close to the coating-substrate interface.
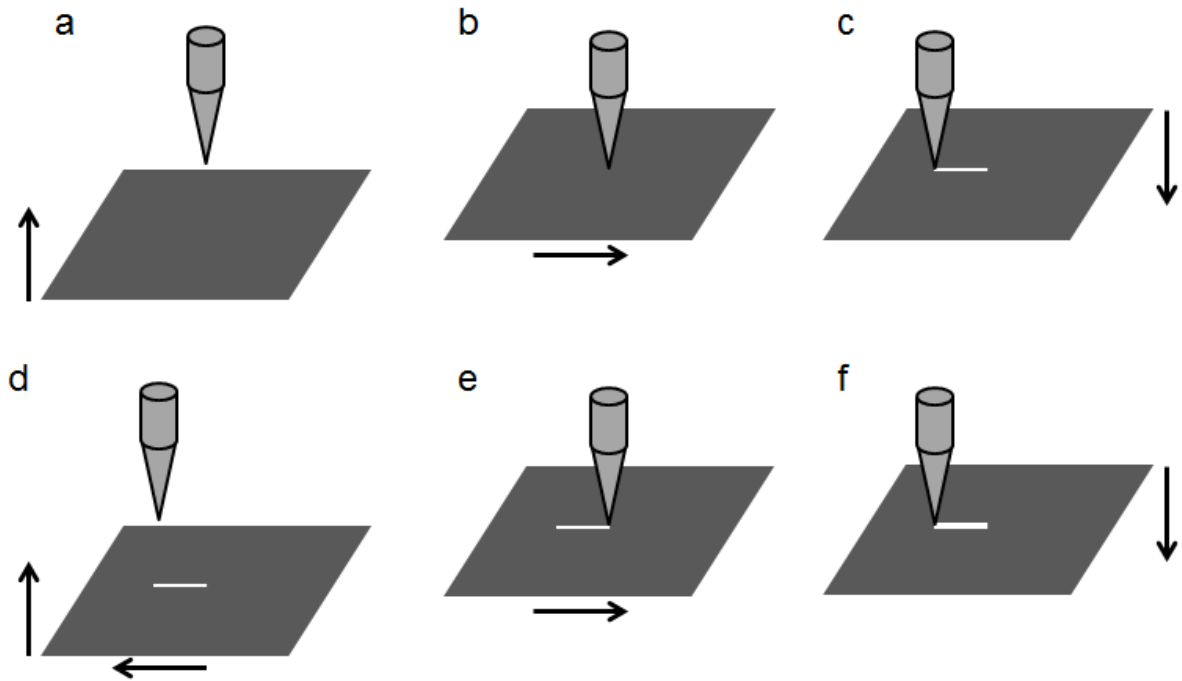
Figure 4. A schematic representation of the first two cycles in an unidirectional nano-wear test. a) sample stage moved to probe to bring into contact b) load is applied; movement of sample stage to create the constant load scratch c) stage is moved away at the end of the scratch d) sample stage restored to exactly the same position and then brought into contact e) load is applied with sample stage movement to create second scratch f) stage moved away; two scratches completed. (after ref 36. A. Singh et al, Acta Materialia 59 (2011) 7311-7324).

Shi and co-workers performed sub-critical load nanowear testing at two load levels to investigate the performance of 1 μm a-C films described above that fail in the progressive load nano-scratch test at a critical load of ~200 mN [16]. The wear test loads were chosen so that the maximum stresses were either within the film (at 50 mN) or the substrate (at 150 mN) so that the additional stress due to the imposed stress field from the scratch reaches the interface for the higher load test. In the lower load wear test the contact is almost completely elastic with residual wear depths under 100 nm. Higher H/E films showed lower residual

depth. An increase in residual wear depth and decrease in scratch recovery with each wear cycle confirm that the low load multi-pass wear test is a fatigue process.
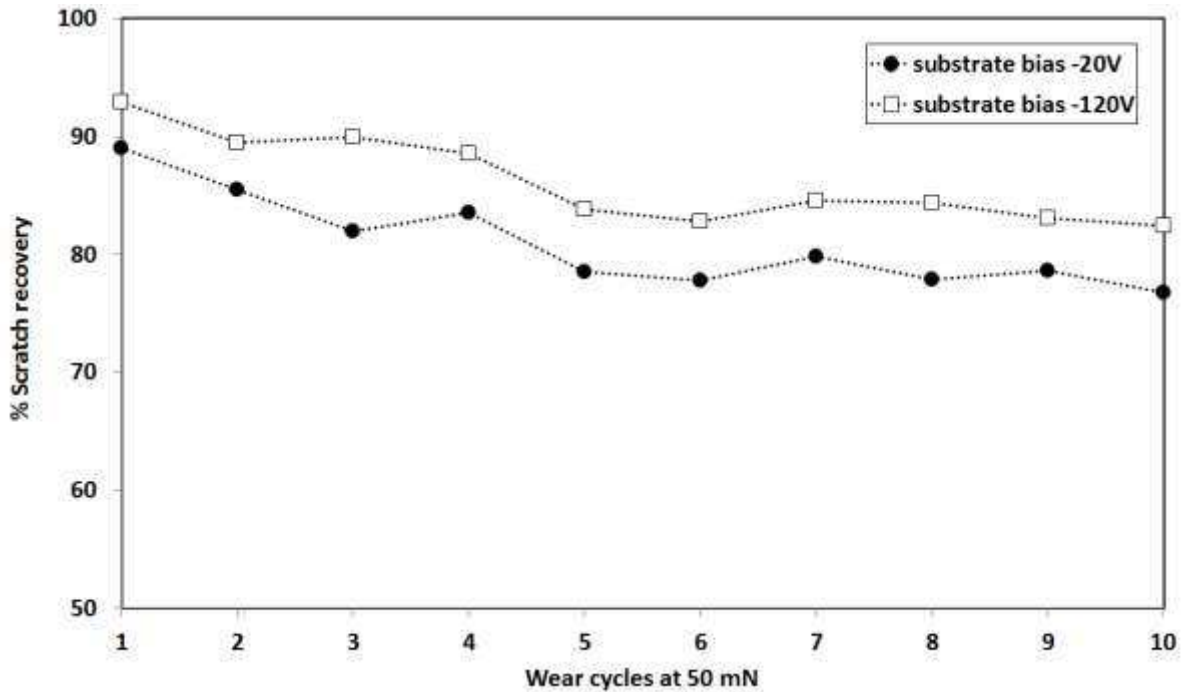

Figure 5. Evolution of scratch recovery and mean pressure during nano-wear test on a-C films at 50 mN using a 4 μm probe

For the film deposited at -20 V substrate bias ($H/E_r = 0.076$), the mean pressure decreases from 9.0 GPa in cycle 1 to 7.9 GPa after 10 cycles. For the film deposited at -120 V substrate bias ($H/E_r = 0.089$), the mean pressure decreases from 13.4 GPa in cycle 1 to 10.6 GPa after 10 cycles.

A reduction in contact pressure through the wear test has also been reported on hardmetals [37], biomedical alloys [27] and TiN films [18]. On 0.5 μm TiN 10 cycles at 100 mN with a 4.4 μm diamond probe caused a decrease in contact pressure from 14.1 GPa to 9.7 GPa and the same

conditions on 1.5 µm TiN led to a reduction from 15.8 GPa to 11 GPa. Gee and Nimishakavi reported that a contact pressure of ~8 GPa decreased to under 1 GPa within 10 cycles of a 20 µm diamond probe at 41.4 mN with contact pressure estimated from measurements of scratch width which dramatically increases.

In marked contrast, when the sub-critical load is a much higher fraction of the critical load the behavior is very different. Nano-wear under these conditions is a very low-cycle fatigue test where plasticity and micro-fracture dominate and the harder films deposited under high bias perform poorly. The behaviour of 1 µm a-C films with a very high ratio of H/E, deposited under high substrate bias, was found to be very strongly dependent on the test conditions, with the films performing well at low load wear but very poorly in more highly loaded contact [16]. They exhibit low critical loads in progressive load scratch tests and when they fail in the nano-wear test there is extensive delamination outside of the scratch track. The combination of nano-wear tests at different loading levels provides information regarding the suitability of the a-C films for contact applications.

3.9. Friction evolution – role of ploughing

The friction force in the nano-scratch test can be deconvoluted into its interfacial and ploughing components so that the interfacial friction can be reported (Eqn. 5):-

$$\mu_{total} = \mu_{interfacial} + \mu_{ploughing} \qquad \text{[Eqn. 5]}$$

The interfacial friction component can be determined by different approaches: (1) performing constant load friction test at very low force where contact is completely elastic and the ploughing contribution is zero (2) performing repetitive scratches to eliminate the ploughing

contribution (3) performing progressive load scratch and extrapolating the low load friction data to zero load. Typically the friction coefficient at yield is of the order of 0.05.

Although frictional measurements are often reported to differ at different length scales it appears that when the extent of deformation is taken into account there is much better agreement. Friction force measurements on TiN in nano-scratch tests are in good agreement with conventional macro-scale scratch testing with a 200 μm diamond probe. Dryda and Sayer reported 0.05 for a range of different 3-5 μm TiN coatings [38]. The values of 0.04 (500 nm TiN) and 0.05 (1500 nm TiN) at 1 mN (R = 3.1 μm) appear to be good estimates for the interfacial component of the sliding friction. As the ploughing contribution increases the total friction increases. The friction coefficient at film failure in the nano-scratch test is ~0.2 consistent with macro-scale determinations of 0.17-0.25 [1,6,38].
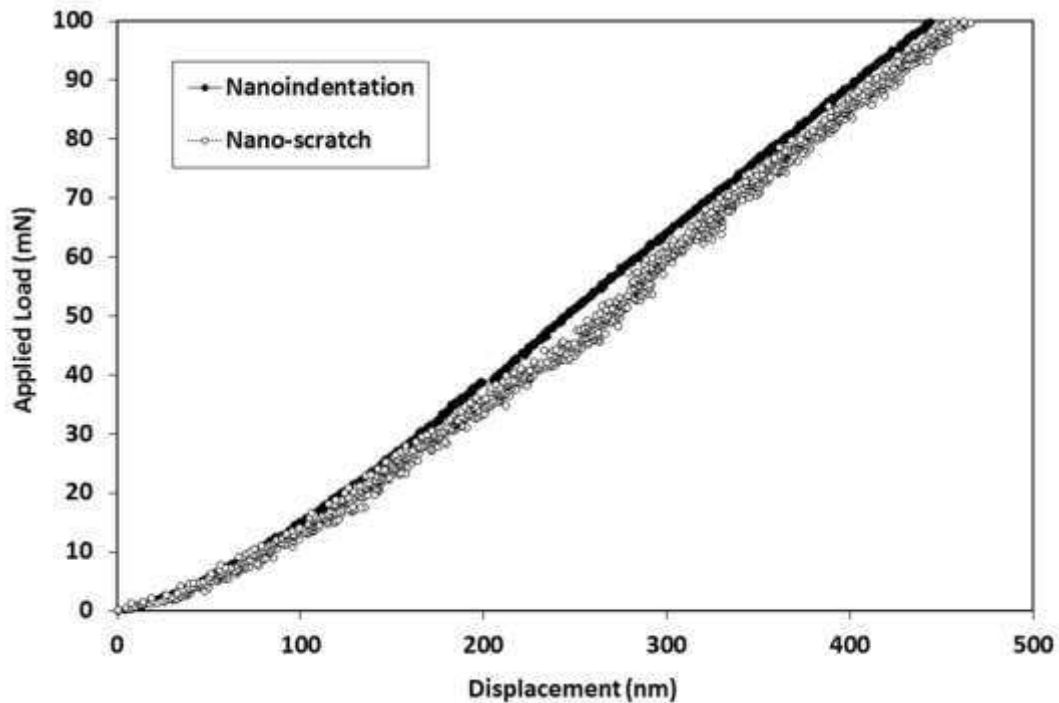
Figure 6. Typical load vs. depth curves in nanoindentation and nano-scratch tests on Si(100) with a 4.6 μm spherical probe

When friction and surface roughness are low the loading curves in indentation and scratch tests can be surprisingly similar [24]. As an illustration of this, Figure 6 shows the response of Si(100) to indentation and scratch testing with the same spherical probe. The friction coefficient at pop-in is low (~0.07), similar to the value of (0.08 ± 0.01) that marks the onset of ploughing in nano-scratching with a 1 μm tip [39].

In contrast, metallic alloys such as 316L stainless steel and Ti6Al4V show a predominantly ductile response to scratching with ploughing and pile-up and debris at the sides of the scratch track, with the onset of chipping events at increasing applied load. Compared to Si(100) the metallic samples have higher friction at comparable load and consequently the deformation during the nano-scratch test is greater than in nanoindentation. The friction, wear depth and mean pressure evolve continually with repetitive scratching of metallic samples.

Table 2 Evolution of friction and mean pressure during nano-wear test on biomedical materials at 30 mN using a 3.7 μm probe

Alloy	Mean friction coefficient in wear cycle 1	Mean friction coefficient in wear cycle 10	Mean pressure in wear cycle 1 (GPa)	Mean pressure in wear cycle 10 (GPa)
CoCr	0.24	0.14	5.9	3.8
316 L steel	0.32	0.17	4.0	2.0
Ti6Al4V	0.37	0.33	5.0	1.4

In the nano-wear test the Hertzian treatment is approximate on these alloys due to their high friction but it can provide a convenient way to estimate contact pressures without the need for post-test imaging and can therefore be used to follow the evolution of contact pressure with repetitive scratching as has been done in Table 2. The contact pressure decreases rapidly due to wear within a few cycles [27]. The increase in the on-load probe depth over the 10 cycle wear test is around 750 nm on the Ti6Al4V but only 100 nm on the CoCr. The Ti6Al4V alloy, which wears the most, consequently shows the largest drop in mean pressure.

The observed frictional behaviour on repetitive sliding is explained by changes to the ploughing component of friction and smoothing of asperities, both of which alter the contact area and therefore can influence the friction [40]. The evolution of friction and wear in the repetitive nano-scratch test can be followed by the parameters μ_1/μ_n and d_1/d_n. For these metals μ_1/μ_n scales with d_1/d_n so that decreasing ploughing contribution results in $\mu(\text{Ti6Al4V}) > \mu(\text{316L stainless steel}) > \mu(\text{CoCr})$. Studies of the relative importance of yield

stress and microstructure on the evolution of friction and wear of metallic materials during micro-scale repetitive sliding have concluded that yield stress plays the dominant role on the evolution of friction as the friction was almost independent of the grain size but decreased with increasing hardness [41-42]. On titanium high friction (μ ~0.4-0.6) was observed virtually independent of grain size. With repetitive scratch testing titanium showed little [42] or no [41] decrease in friction coefficient, and in the nano-scratch test the decrease in friction was much less on Ti6Al4V than on either CoCr or 316L stainless steel. This is explained by a lower scan-on-scan decrease in the ploughing contribution on pure Ti and the Ti alloy. H/E can prove a more reliable parameter than hardness in predicting the sliding wear resistance of coated systems [43]. For the biomedical alloys it correlates with the extent of scratch recovery and the elastic recovery in nanoindentation. In the repetitive nano-scratches it appears that both mechanical and interfacial properties can influence the wear behavior. With continued scratch passes the samples with lower hardness and higher friction, i.e. titanium alloy and stainless steel, show higher and more variable wear than the CoCr alloy. The different evolution in friction and wear on stainless steel, CoCr and TiAl4V may be related to differences in their stacking fault energies. The titanium alloy has a much higher stacking fault energy than either CoCr or stainless steel and does not work harden to the same degree, resulting in little reduction in ploughing and friction on repetitive nano-scratching.
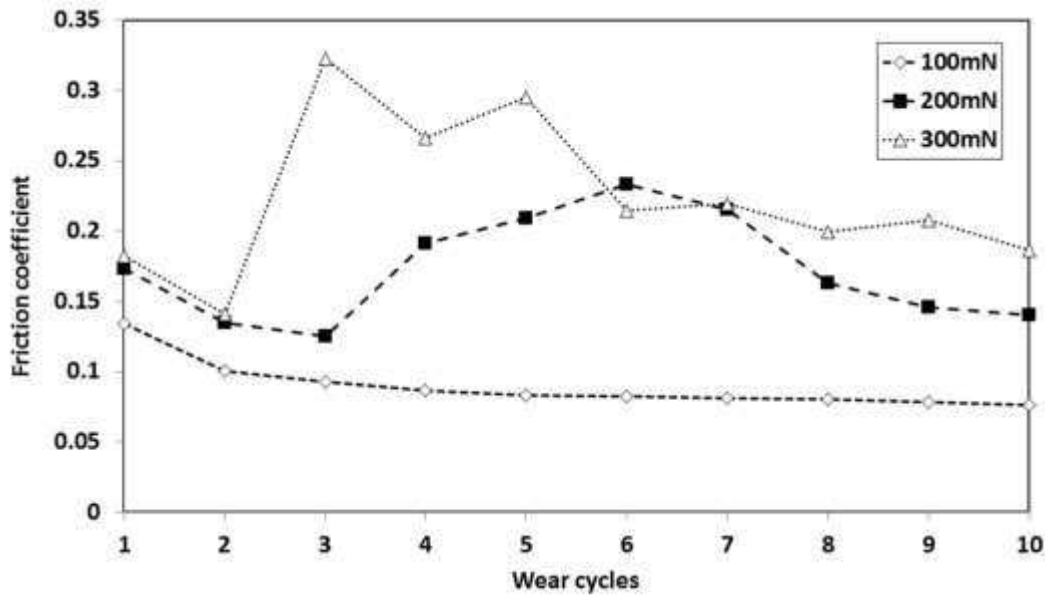
Figure 7. Variation in friction with number of wear cycles

In the nano-wear testing of thin films, the friction force can be very sensitive to the onset of failure, unless the failure occurs behind the moving probe. Figure 7 shows the evolution of the friction coefficient with wear cycles at 100-300 mN for 1500 nm TiN on M42 steel being scratched with a 4.4 μm diamond probe. With repeat scratching the friction coefficient initially decreases due to a reduction in the ploughing component as described above for metallic samples. The onset of coating failure was marked by a sudden sharp increase in friction during a single wear cycle (cycle 2 at 300 mN and cycle 3 at 200 mN in figure 18) which is accompanied by an inflexion in the depth vs. wear cycle. After the abrupt increase in friction at film failure the friction decreases with continued scratch cycles as failure debris is removed from the scratch track.

26

4. Conclusions

In this paper a review of recent progress in nano-scratch testing was carried out and the following conclusions can be drawn:

1. The critical load in nano-scratch test can be influenced by extrinsic and intrinsic factors. In addition, the mechanical properties of the coating and lateral stiffness of the instrument can also play an important role in nano-scratch experiments.

2. It has been observed that there was considerably less sensitivity to scan speed and loading rate in nano-scratch experiments than in macro-scale scratch testing. The results suggest also that nano-scratch tests under significantly different loading conditions can be compared directly.

3. The nano-scratch 3-scan procedure involving a sequence of topography scan, progressive scratch scan and topography scan enables identification of failure mechanisms and the role of stress in tested materials. Using this method, it is also possible to determine the critical load for the onset of non-elastic deformation.

4. Investigation of influence of probe radius and geometry revealed that periodic calibration of the indenter radius by nanoindentation is necessary to determine the effective radius and ensure the calibration remains accurate. It has been also established that ~5 μm represents an effective choice of end probe radius ensuring that coating failure is observed within the force range of several commercial instruments but without risking rapid blunting of the indenter due to repeat scanning.

5. An approach based on indentation data enabling estimation of the contact pressure required for the failure of the film has been discussed. The approach can be used in the nano-scratch test, although it becomes less valid as the geometry moves away from Hertzian conditions due to increasing friction or plasticity.

6. Impact of surface roughness on nano-scratch experiments has been discussed and it has been shown that the critical load for delamination failure was dependent on scratch orientation relative to polishing marks on the surface made prior to coating deposition. Coating failure was more gradual when the scratch direction was either parallel to or aligned at an intermediate angle to the grinding grooves than when it was perpendicular.

7. It has been shown that the film thickness is a key parameter influencing the critical load in the nano-scratch test, however the relationship between film thickness and critical load can be quite complex in practice. For optimum durability in highly loaded sliding contact, when films are deposited to around 1 µm thickness they should not be designed to be as hard and have as high a ratio H/E_r as possible.

8. When compared to progressive load nano-scratch testing, repetitive nano-wear testing has the advantage that the load can be varied to tune the maximum von Mises stress to be close to the coating-substrate interface. Nano-wear experiments can also be much more informative regarding the influence of thin film stress leading to poor adhesion than single scratch tests.

9. The friction force in the nano-scratch test can be deconvoluted into its interfacial and ploughing components. It has been shown however that the impact of ploughing on friction has a complex mechanism and depends strongly on mechanical properties of tested materials.

References

1. M. Larsson, M. Olsson, P. Hedenqvist, S. Hogmark: 'Mechanisms of coating failure as demonstrated by scratch and indentation testing of TiN coated HSS – On the influence of coating thickness, substrate hardness and surface topography', Surf. Eng., 2000, **16**, 436-44.

2. H. Ichimura and Y. Ishii: 'Effects of indenter radius on the critical load in scratch testing', Surf. Coat. Technol., 2003, **165**, 1-7.

3. K. Holmberg, H. Ronkainen, A. Laukkanen and K. Wallin: 'Friction and wear of coated surfaces – scales, modelling and tribomechanisms', Surf. Coat. Technol., 2007, **202**, 1034-49.

4. K. Holmberg, H. Ronkainen, A. Laukkanen, K. Wallin, A. Erdemir and O. Eryilmaz: 'Tribological analysis of TiN and DLC coated contacts by 3D FEM modelling and stress simulation', Wear, 2008, **264**, 877-84.

5. P.A. Steinmann, Y. Tardy and H.E. Hintermann: 'Adhesion testing by the scratch test method: influence of intrinsic and extrinsic parameters on the critical load', Thin Solid Films, 1987, **154**, 333-49.

6. H. Ollendorf and D. Schneider: 'A comparative study of adhesion test methods for hard coatings', Surf. Coat. Technol., 1999, **113**, 86-102.

7. S.J. Bull and D.S. Rickerby: 'New developments in the modelling of the hardness and scratch adhesion of thin films' Surf. Coat. Technol., 1990, **42**, 149-64.

8. P.J. Burnett and D.S. Rickerby: 'The relationship between hardness and scratch adhesion', Thin Solid Films, 1987, **154**, 403-16.

9. S.J. Bull: 'Failure modes in scratch adhesion testing', Surf. Coat. Technol., 1991, **50**, 25-32.

10. B.D. Beake, V.M. Vishnyakov, R. Valizadeh and J.S. Colligon: 'Influence of mechanical properties on the nanoscratch behaviour of hard nanocomposite TiN/Si_3N_4 coatings on Si', J. Phys. D: Appl. Phys., 2006, **39**, 1392-1397.

11. B.D. Beake, V.M. Vishnyakov, and A.J. Harris:- 'Relationship between mechanical properties of thin nitride-based films and their behaviour in nano-scratch tests', Tribol. Int., 2011, 44, 468.

12. S. Roy, E. Darque-Ceretti, E. Felder, F. Raynal, I. Bispo: 'Experimental analysis and finite element modelling of nano-scratch test applied on 40–120 nm SiCN thin films deposited on Cu/Si substrate', Thin Solid Films, 2010, **518**, 3859-3865.

13. W. Tang, X. Weng, L. Deng, K. Xu and J. Lu: 'Nano-scratch experiments of Au/NiCr multi-layered films for microwave integrated circuits', Surf. Coat. Technol., 2007, **201**, 5664-5666.

14. B.D. Beake, S.P. Lau: 'Nanotribological and nanomechanical properties of 5-80 nm tetrahedral amorphous carbon films on silicon', Diam. Relat. Mater., **14**, 1535-1542.

15. B.D. Beake, A.A Ogwu and T. Wagner:'Influence of experimental factors and film thickness on the measured critical load in the nanoscratch test', Mater. Sci. Eng. A 2006, **423**, 70-73.

16. B. Shi, J.L. Sullivan and B.D. Beake: 'An investigation into which factors control the nanotribological behaviour of thin sputtered carbon films', J. Phys. D: Appl. Phys., 2008, **41**, 045303.

17. B.D. Beake, S.R. Goodes and B. Shi:'Nanomechanical and nanotribological testing of ultra-thin carbon-based and MoST films for increased MEMS durability', J. Phys. D: Appl. Phys., 2009, **42**, 065301.

18. B.D. Beake, B. Shi and J.L. Sullivan, J.L:'Nanoscratch and nanowear testing of TiN coatings on M42 steel', Tribology, 2011, **5**, 141-147.

19. B.D. Beake, M.I. Davies, T.W. Liskiewicz, V.M. Vishnyakov and S.R. Goodes: 'Nano-scratch, nanoindentation and fretting tests of 5–80nm ta-C films on Si(100)', Wear, Available online 4 February 2013, 10.1016/j.wear.2013.01.073.

20. S.M. Noh, J.W. Lee, J.H. Nam, J.M. Park and H.W. Jung: 'Analysis of scratch characteristics of automotive clearcoats containing silane modified blocked isocyanates via carwash and nano-scratch tests', Progress in Organic Coatings, 2012, 74, 192-203,

21. W.-E. Fu, C.-C.A. Chen, K.-W. Huang, Y.-Q. Chang, T.-Y. Lin, C.-S. Chang and J.-S. Chen: 'Nano-scratch evaluations of copper chemical mechanical polishing', Thin Solid Films, 2013, **529**, 306-311,

22. S. Gao, Z. Cai, S. Huang, L. Qian and H. Yu: 'Nano-scratch behavior of human root canal wall dentin lubricated with EDTA pastes' Tribol. Int., 2013, **63**, 169-176

23. A. Karimzadeh and M.R. Ayatollahi: 'Investigation of mechanical and tribological properties of bone cement by nano-indentation and nano-scratch experiments' Polymer Testing, 2012, **31**, 828-833.

24. B.D. Beake, T.W. Liskiewicz and J.F. Smith: 'Deformation of Si(100) in spherical contacts – Comparison of nano-fretting and nano-scratch tests with nano-indentation', Surf. Coat. Technol., 2011, **206**, 1921-1926.

25. NANOINDENT Creating and disseminating novel nanomechanical characterisation techniques and Standards Part funded by the European Community's Seventh Framework Programme (FP7/2007-2013) under grant agreement NMP3-CA-2008-218659.FP7

26. NANOINDENT-PLUS project Standardising the nano-scratch test is being part-funded from the European Community's Seventh Framework Programme (FP7/2007-2013) under grant agreement NMP-2012-CSA-6-319208.

27. B.D. Beake and T.W. Liskiewicz: 'Comparison of nano-fretting and nano-scratch tests on biomedical materials', Tribol. Int., Available online 24 August 2012, 10.1016/j.triboint.2012.08.007.

28. T.W. Wu, R.A. Burn, M.M. Chen and P.S. Alexopoulos, Mat. Res. Soc. Symp. Proc., 1989, **130**, 117-122.

29. T.W. Wu: J. Mater. Res., 1991, **6**, 407.

30. I.D. Spary, A.J. Bushby and N.M. Jennett: 'On the indentation size effect in spherical indentation', Philos. Mag., 2006, **86**, 5581-5593.

31. X.D. Hou A.J. Bushby and N.M. Jennett: 'Study of the interaction between indentation size effect and Hall-Petch effect with spherical indenters on annealed polycrystalline copper', J. Phys. D: Appl. Phys., 2008, **41**, 074006 (7pp).

32. X.D. Hou, and N.M. Jennett: 'Application of a modified slip-distance theory to the indentation of single-crystal and polycrystalline copper to model the interactions between indentation size and structure size effects', Acta. Mater., 2012, **60**, 4128-4135.

33. M.T. Raimondi, P. Vena and R. Pietrabissa: 'Quantitative evaluation of the prosthetic head damage induced by microscopic third-body particles in total hip replacement', J. Biomed. Mater. Res. (Appl. Biomater.), 2001, **58**, 436-448.

34. M. Mirghany and Z.M. Jin: 'Prediction of scratch resistance of cobalt chromium alloy bearing surface, articulating against ultra-high molecular weight polyethylene, due to third body wear particles', Proc IMechE: H, 2004, 218, 41-50.

35. J.R. Goldberg and J.E. Gilbert: 'Electrochemical response of CoCrMo to high-speed fracture of its metal oxide using an electrochemical scratch test method', J. Biomed. Mater. Res., 1997, **37**, 421-431.

36. A. Singh, M. Dao, L. Lu and S. Suresh: 'Deformation, structural changes and damage evolution in nanotwinned copper under repeated frictional contact sliding', Acta. Mater., 2011, **59**, 7311-7324.

37. M.G. Gee and L. Nimishakavi, Int. J. Refract. Hard. Mater., 2011, **29**, 1-9.

38. K. Dryda and M. Sayer, Thin Solid Films, 1999, **355-356**, 277-283.

39. B. Bhushan, B.K. Gupta and M.H. Azarian, Wear, 1995, **181-183**, 743.

40. S. Achanta, T.W. Liskiewicz, D. Drees and J.-P. Celis: 'Friction mechanisms at the micro-scale', Tribol. Int., 2009, **42**, 1792-1799.

41. C.T. Wang, N. Gao, M.G. Gee, R.J.K. Wood and T.G. Langdon: 'Effect of grain size on the micro-tribological behaviour of pure titanium processed by high-pressure torsion', Wear, 2012, **280-281**, 28-35.

42. T. Hanlon, A.H. Chokshi, S. Manoharan and S. Suresh: 'Effects of grain refinement and strength on friction and damage evolution under repeated sliding contact in nanostructured metals' Int. J. Fatigue 2005, **27**, 1159-1163.

43. A. Leyland and A. Matthews: 'On the significance of the H/E ratio in wear control: a nanocomposite coating approach to optimised tribological behaviour', Wear, 2000, **246**, 1.